Virus Research 338 (2023) 199240

Contents lists available at ScienceDirect

Virus Research

journal homepage: www.elsevier.com/locate/virusres

HMGB1 Release Induced by EV71 Infection Exacerbates Blood-Brain Barrier Disruption via VE-cadherin Phosphorylation

Qiao You [a,1], Jing Wu [a,1], Ye Liu [b], Fang Zhang [c], Na Jiang [a], Xiaoyan Tian [a], Yurong Cai [d], Enhui Yang [e], Ruining Lyu [a], Nan Zheng [a], Deyan Chen [a,*], Zhiwei Wu [d,f,g,*]

[a] Center for Public Health Research, Medical School of Nanjing University, Nanjing, China
[b] China Department of Ophthalmology, Tianjin First Central Hospital, Tianjin, China
[c] Department of Burn and Plastic Surgery, Affiliated Hospital of Zunyi Medical University, Zunyi, China
[d] School of Life Sciences, Ningxia University, Yinchuan, PR China
[e] Department of Child Healthcare, Wenzhou People's Hospital, Wenzhou, Zhejiang, China
[f] State Key Laboratory of Analytical Chemistry for Life Science, Nanjing University, Nanjing, China
[g] Jiangsu Key Laboratory of Molecular Medicine, Medical School of Nanjing University, Nanjing, China

ARTICLE INFO

Keywords:
HMGB1
EV71
BBB
inflammation
VE-cadherin phosphorylation

ABSTRACT

Purpose: EV71 (Enterovirus 71) is a major causative agent of the outbreaks of HFMD (hand, foot, and mouth disease), which is associated with neurological damage caused by permeability disruption of BBB (blood-brain barrier). HMGB1 (high-mobility group box 1) is a widely expressed nuclear protein that triggers host inflammatory responses. Our work aimed to explore the function of HMGB1 in EV71 infection and its contributions to EV71-related BBB damage.

Methods: HeLa cells, HT-29 cells and AG6 mice were used to explore the translocation of HMGB1 in EV71 infection *in vitro* and *in vivo*. The roles of released HMGB1 on EV71 replication and associated inflammatory cytokines were investigated using recombinant HMGB1 in HeLa cells. The mechanisms of released HMGB1 in EV71-induced BBB injury were explored using recombinant HMGB1 and anti-HMGB1 neutralizing antibodies in monolayer HCMECs (immortalized human brain microvascular endothelial cells) and AG6 mice brain.

Results: EV71 induced HMGB1 nucleocytoplasmic translocation and extracellular release *in vitro* and *in vivo*. Released HMGB1 acted as an inflammatory mediator in EV71 infection rather than affecting viral replication *in vitro*. Released HMGB1 disrupted BBB integrity by enhancing VE-cadherin phosphorylation at tyrosine 685 in HCMECs, and reducing total VE-cadherin levels in HCMECs and AG6 mice in EV71 infection. And released HMGB1 induced an increase in activated astrocytes. Neutralization of HMGB1 reversed the increased endothelial hyperpermeability and phosphorylation of VE-cadherin in HCMECs.

Conclusion: The inflammatory mediator HMGB1 released by EV71 exacerbated BBB disruption by enhancing VE-cadherin phosphorylation, which in turn aggravated EV71-induced neuroinflammation.

1. Introduction

EV71 (*Enterovirus 71*) is a positive-strand RNA virus from the genus *Enterovirus* in the family *Picornaviridae*, which is a major causative agent of HFMD (hand, foot, and mouth disease). (Solomon et al., 2010) HFMD generally occurs to children younger than 5 years old and cause neurological syndrome. (Zhu et al., 2014, Chang et al., 2007, Crabol et al., 2017, Ooi et al., 2010, Cox and Levent, 2018) Encephalitis and brainstem encephalitis are the most frequent manifestations after EV71 infection of CNS (central nervous system). Disruption of the BBB (blood-brain barrier) is closely associated with the inflammatory responses in the CNS. (Sweeney et al., 2019, Nishibori et al., 2019,

Abbreviations: EV71, enterovirus 71; HFMD, hand, foot, and mouth disease; BBB, blood-brain barrier; HMGB1, high-mobility group box 1; CNS, central nervous system; hpi, hours post infection; dpi, days post infection; MOI, multiplicity of infection; i.p, intraperitoneal injection; GFAP, glial fibrillary acidic protein; Iba1, ionized calcium-binding adapter molecule 1; Tyr^{685}, tyrosine 685.

* Corresponding authors at: Medical School of Nanjing University, Nanjing, 210093, China.
E-mail addresses: chendeyan@nju.edu.cn (D. Chen), wzhw@nju.edu.cn (Z. Wu).

[1] These authors contributed equally to this work.

https://doi.org/10.1016/j.virusres.2023.199240
Received 31 August 2023; Received in revised form 9 October 2023; Accepted 10 October 2023

Nishibori et al., 2020) The BBB, mainly composed of endothelial cells, protects the CNS from toxins and invading pathogens in the peripheral blood circulation. (Chang et al., 2007, Koyuncu et al., 2013, Obermeier et al., 2013) Tight junctions (TJs) and adhering junctions (AJs) constitute the integrity of the BBB, and homophilic interactions between cadherins such as VE-cadherin are considered as the prerequisite for the establishment of TJs. (Dejana and Orsenigo, 2013, Liebner et al., 2018) Loss of TJs and AJs leads to the activation of astrocytes and microglia, which aggravate inflammation in the CNS. (Colombo and Farina, 2016, Linnerbauer et al., 2020, Colonna and Butovsky, 2017, Sweeney et al., 2018) Thus, it is crucial to identify risk factors for EV71-cause BBB damage.

HMGB1, a highly conserved nuclear protein, has been reported to regulate viral replication and trigger the inflammatory responses in a variety of viral infections. (Yu et al., 2015, Qu et al., 2018, Stros, 2010) Emerging evidence suggests that HMGB1 could be actively released by immunologically competent cells, or released by necrotic cells to response to stressors. (Wang et al., 1999, Ding et al., 2021, Andersson and Tracey, 2011) As a late-released inflammatory factor, HMGB1 strongly induces overexpression of a large number of proinflammatory cytokines, leading to the persistence of dangerous inflammation. (Wang et al., 1999, Ding et al., 2021, Andersson et al., 2020) Recently, high levels of HMGB1 has been observed in EV71-related severe and critical HFMD cases, which are positively correlated with the alteration of IL-6 and TNF-α concentrations. (Zheng et al., 2017) Increasing evidence suggests that HMGB1 is involved in BBB damage induced by brain-injury diseases as well as endotoxin-inflammation-induced encephalitis, implying that released HMGB1 can play a very important role in brain injury by disrupting the BBB. (Nishibori et al., 2020, Nosaka et al., 2018, Zhang et al., 2011, Wang et al., 2020) However, the roles of HMGB1 in EV71 infection are not clear, and the relationships between HMGB1 and BBB integrity during EV71 infection are yet to be explored.

In this study, we showed that the release of HMGB1 *in vitro* and *in vivo* was increased after EV71 infection. Then we found that released HMGB1 acted as an inflammatory mediator in EV71 infection rather than affecting viral replication. Furthermore, we demonstrated that released HMGB1 enhanced BBB permeability by enhancing VE-cadherin phosphorylation, resulting in CNS inflammation.

2. Materials and methods

2.1. Cells and virus

HT-29 cells (human colorectal cell lines), HeLa cells (human epithelial carcinoma cell lines) and Vero cells (african green monkey kidney epithelial cells) were purchased from the American Type Culture Collection. HCMECs (immortalized human brain endothelial cell lines) were purchased from Millipore (USA). Vero cells, HeLa cells and HT-29 cells were grown in high-glucose DMEM (HyClone, Logan, UT, USA) plus 10% or 2% FBS (Gibco, Carlsbad, CA, USA). HCMECs were grown in complete ECM plus 5% FBS, Endothelial Cell Growth Supplement (ECGS) and antibiotic solution (P/S) (#1001, ScienCell Research Laboratories, San Diego, California, USA). The above cells were incubated at 37°C with a 5% CO_2 humidified atmosphere.

The BrCr strain of EV71 used in this study was obtained from Dr. Bin Wu. (Wang et al., 2019) Vero cells were used for EV71 multiplication. The virus titers were calculated as the 50% tissue culture infectious dose (TCID50) using the Reed–Munch method as previously described. (Wang et al., 2019, Feng et al., 2017)

2.2. RNA extraction and quantitative real-time PCR

RNA was extracted from cells samples using TRIzol reagent (Life Technologies, Carlsbad, USA). Reverse-transcribed cDNA was synthesized using the PrimeScript RT Reagent Kit (TaKaRa, Kyoto, Japan). Quantitative real-time PCR was performed with SYBR green qPCR Master mix (Vazyme biotech, Nanjing, China) under Applied Biosystems 7500 system. All the used primers were listed in **Supplementary Table 1**. The mRNA levels were normalized to GAPDH, and the analysis was performed by $2^{-\Delta\Delta Ct}$ method.

2.3. Western blot assay

The cells were collected and then lysed using RIPA (sc-364162A, Santa Cruz, Dallas, USA) containing phosphatase inhibitors (Beyotime, Shanghai, China). The concentration of extracted protein was determined by Bicinchoninic Acid (BCA) Protein Assay Kit (Pierce, Thermo, Massachusetts, USA) as described. (Chen et al., 2018) Extracted proteins were separated by sodium dodecyl sulfate-polyacrylamide gel electrophoresis (SDS-PAGE) (BIO-RAD, Hercules, USA) and transferred onto polyvinylidene (PVDF) membranes (Millipore, Massachusetts, and USA). After blocking for 1 h, the membranes were incubated with specific antibodies at 4°C about 12 h. The IRDye 800 goat anti-mouse IgG or IRDye 680 donkey anti-rabbit IgG (LI-COR Bioscience, Lincoln, USA) were incubated with the membranes for 60 min as discribed. (Fu et al., 2019) Protein signals were detected by Odyssey Infrared Imaging System, and the band intensity of proteins was quantified by Image J software. The used antibodies are listed in **Supplementary Table 2**.

2.4. ELISA

HMGB1 in cell-free supernatants was determined by a HMGB1 Detection ELISA Kit (6010, Chondrex, Washington, USA), and HMGB1 in mice serum was quantitated by a Mouse HMGB1 ELISA Kit (E-EL-M0676c, Elabscience, Wuhan, China) according to the manufacturers' instructions. IL-6, IFN-γ, IL-2, IL-13, IL-8, IL-10, 1L-12, IL-1β, IL-4 and TNF-α in cell-free supernatants from EV71-infected HeLa cells were quantified by Luminex-based multiplex protein arrays (BIO-RAD, CA, USA) according to the manufacturers' instructions.

2.5. Immunofluorescence assay

4% Paraformaldehyde (Servicebio, Wuhan, China) was used to fix cells about 15 min and 0.5% Triton X-100 was performed to permeabilize cells about 15 min, and followed by blocking with 2% bovine serum albumin about 1.5 h. Then the cells were incubated with specific antibodies at 4°C for 12 h. Subsequently, the cells were incubated with Alexa Fluro 594-labeled donkey anti-rabbit IgG or Alexa Fluro 488-labeled goat anti-mouse IgG about 1 h. And then DAPI was used to stain cell nucleus. The cells were observed and imaged by Olympus Fluoview FV3000 as previously described. (Wang et al., 2021) The used antibodies are listed in **Supplementary Table 2**.

2.6. Cell viability

The cells of HeLa and HT-29 were incubated with EV71 for the indicated time, then the cell counting kit-8 (Invigentech, California, USA) was used to detect the surviving cells according to the manufacturers' instructions.

2.7. In vitro BBB model

8×10^4 HCMECs were seeded into Costar Transwell inserts (CLS3413, Corning, NY, USA) coating with collagen (0.1 mg/mL) and cultured in complete ECM for 4-6 days to form mature monolayers. Then 500 μL of DMEM was added to each of the upper and lower chambers for permeability testing for 4 h. Then, the liquid level in the lower chamber was checked for a drop to verify the success of the model. After the leakage-test, EV71 or HMGB1 protein (10326-H08H, Sino Biological, Beijng, China) was added to the mature cell monolayer. Then after 24 h incubation, the PBS was used to replace the media. For BBB permeability testing, fluorescein sodium salt (10 μg/mL) was incubated in the upper

chamber of monolayers about 30 min, then the absorbance at a wavelength of 490 nm of the liquid from the lower chamber was measured by spectrophotometer.

2.8. In vitro HMGB1 neutralization BBB model

HeLa cells were infected with EV71 in the presence of anti-HMGB1 neutralizing antibody (SQab20175, arigo Biolaboratories, Taiwan, China) or control IgG antibody (ARG65345, arigo Biolaboratories, Taiwan, China). After 24 h incubation, the cell supernatants were collected and then treated with UV (Ultraviolet light) for 30 min in sterile dish. Then, the treated cell supernatants were added to Vero cells to detect if there are still active viral particles of EV71. After the test, the cell supernatants were added to *in vitro* BBB model and HCMECs in 6-well plates.

2.9. Ethics approval and consent to participate

The mice named AG6, who lacking interferon receptor, were donated by Professor Qibin Leng (Shanghai, China). The mice were housed in controlled conditions (no specific pathogen, 12-h light/dark cycle). The animal experiments were approved by Animal Care and Use Committee of Nanjing University. All protocols in this study were conducted in accordance with the animal behavioral guidelines using protocols approved by the institutional animal care committee.

2.10. In vivo EV71 infection model

2-week-old AG6 mice (n = 4) were infected with 1.76×10^7 PFU of EV71. On day 4 of EV71 post-infection, the serum from mice was collected for detecting HMGB1 levels by ELISA, and the intestine tissues were harvested and stained with HMGB1 antibody and EV71 VP1 antibody in immunofluorescence assay.

2.11. In vivo BBB model

AG6 mice at the age of 2 weeks were intraperitoneally infected with EV71 at 1.76×10^7 PFU/mouse and HMGB1 protein at 5 μg/mouse (n = 5) or PBS (n = 4), Mock-infected mice were injected intraperitoneally with HMGB1 protein at 5 μg/mouse (n = 4) or PBS (n = 5). On day 7 of post-infection, Evans blue (50 mg/kg) was used to circulate in the whole body for 1 h. The mice were anesthetized, perfused with 0.9% saline supplemented with 5 mM EDTA, and fixed with 4% paraformaldehyde. The concentration of Evans blue in mice brain was determined as described before. (Xu et al., 2021) Briefly, half of the mouse brain was weighted, homogenized, and then mixed with formamide (Invitrogen, California, USA) at 60°C about 12 h. Lastly, they were measured at 620 nm. Another half of the brain was paraffin embedded, sectioned, and stained with EV71 VP1 antibody, GFAP antibody, Iba1 antibody and VE-cadherin antibody in immunofluorescence assay.

2.12. Statistical analysis

All statistical analyses were performed using *GraphPad Prism*, version 8.0 (GraphPad Software, San Diego, CA, USA). Except for the animal studies (one time), each experiment was repeated at least 3 times. The results were shown as mean ± standard error of the mean (SEM) and were compared using *Student t*-tests and *one-way ANOVA* followed by a *SNK-q test*. $^*P < 0.05$ represents the statistical significance (ns, no significant, $^{**}P < 0.01$, $^{***}P < 0.001$ and $^{****}P < 0.0001$).

3. Results

3.1. EV71 induces HMGB1 release in vitro and in vivo

To investigate the relationship between EV71 infection and HMGB1 release, we established the EV71 infection model *in vitro* and *in vivo*. HMGB1 mRNA expression was significantly increased by 1.6-fold at 16 hpi, and 1.9-fold at 24 hpi as compared to uninfected HeLa cells (Fig. 1**A**), in which the viability of EV71-infected cells was not affected (**Figure S1A** and **B**). However, the total HMGB1 protein levels significantly declined by 34% and 47% at 16 hpi and 24 hpi, respectively (Fig. 1**B** and **C**). The similar results were obtained in HT-29 cells (Fig. 1**D-F**). We further found that HMGB1 levels in culture supernatants exhibited 1.4 ~ 18.6-fold increase in EV71-infected HeLa cells and 2 ~ 11.8-fold increase in HT-29 cells (Fig. 1**G** and **H**), suggesting that HMGB1 was released upon EV71 infection. Furthermore, we observed that HMGB1 was predominantly present in the nucleus of uninfected cells, while in contrast it appeared in the cytoplasm of ~ 95% EV71-infected cells with concomitant reduction in the nucleus at 12 hpi (Fig. 1**I**), suggesting that EV71 induced HMGB1 cytoplasmic translocation in the early stages of viral infection.

AG6 mice are more susceptible to CNS damage in response to viral infection. (Zhou et al., 2023) We next investigated the release of HMGB1 in EV71-infected AG6 mice (Fig. 2**A**). We found that about ~83% HMGB1 protein was released from the nuclei of intestinal cells of EV71-infected mice (Fig. 2**B**), and about 3-fold increase of HMGB1 in the serum of EV71-infected mice (6.00 ± 2.16 ng/mL) as compared to uninfected mice (2.73 ± 0.36 ng/mL) (Fig. 2**C**). Taken together, the results suggested that EV71 infection induced HMGB1 cytoplasmic translocation and then the cytoplasmic HMGB1 was released into the extracellular space.

3.2. Released HMGB1 acts as a proinflammatory mediator in EV71 infection

Next, we used recombinant HMGB1 to mimic released HMGB1 to treat cells and analyzed the effect on EV71 replication. We found that HMGB1 protein treatment at 50 or 500 ng/mL did not affect EV71 replication *in vitro* (Fig. 3**A** and **B**), which implied that HMGB1 did not affect viral replication. And we also excluded the effect of anti-HMGB1 neutralizing antibody on EV71 replication (**Figure S1C**). HMGB1 has been reported as a proinflammatory mediator in multiple diseases. (Andersson and Tracey, 2011) Therefore, we detected the release of a series of inflammatory cytokines including IL-6, IFN-γ, IL-2, IL-13, IL-8, IL-10, 1L-12, IL-1β, IL-4 and TNF-α in EV71-infected HeLa cells. We found that EV71 significantly induced the release of IL-6 and IL-8 (Fig. 3**C**). And EV71 infection induced a 2-fold increase of IL-6 mRNA levels (Fig. 3**D**) and a 2.2-fold increase of IL-8 mRNA levels (Fig. 3**E**). 50 or 500 ng/mL of HMGB1 protein markedly increased the expression of IL-8 mRNA about 2-fold, but not IL-6 (Fig. 3**D** and **E**). These data suggested that released HMGB1 acted as a proinflammatory mediator in EV71 infection.

3.3. Released HMGB1 exacerbates EV71-induced BBB disruption and CNS inflammation

To explore the roles of HMGB1 in BBB permeability during EV71 infection, we established an *in vitro* BBB model (Fig. 4**A**). We found that EV71 infection significantly increased the permeability of HCMECs monolayers by 2.6-fold, and HMGB1 protein stimulation markedly increased BBB permeability by 10% with EV71 infection (Fig. 4**B**). Furthermore, we used conditioned medium containing HMGB1 from EV71-infected HeLa cells to explore the role of released HMGB1 on BBB permeability in an *in vitro* HMGB1 neutralization BBB model (Fig. 4**C**). UV radiation was used to inactivate infectious virions to avoid the effect of free EV71 particles (Fig. 4**D**). We found that released HMGB1 induced 1.2-fold increase in the permeability of EV71-infected HCMEC monolayer cells, and anti-HMGB1 neutralizing antibody (anti-HMGB1) alleviated 50% of the leakage (Fig. 4**E**), which suggested that released HMGB1 exacerbated BBB disruption *in vitro*.

2-week-old AG6 mice were infected with EV71 and stimulated with

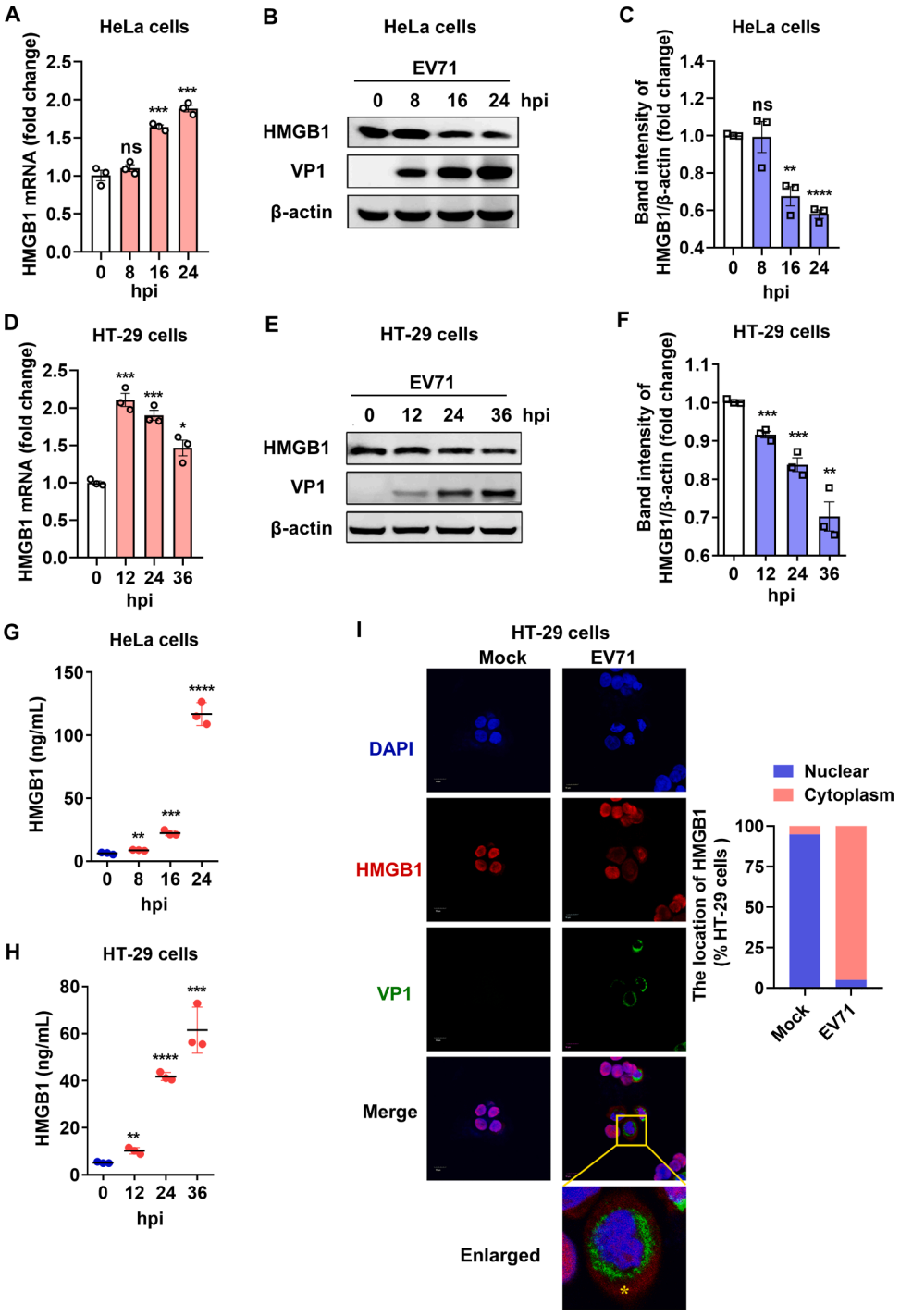

Fig. 1. HMGB1 release is induced by EV71 infection *in vitro*.
(A) HeLa cells were infected with EV71 (hpi = 0, 8, 16, 24) at an MOI of 0.3, then cells were harvested and the HMGB1 mRNA levels were quantified by quantitative real-time PCR, normalized against GAPDH. **(B)** HeLa cells were infected with EV71 (0, 8, 16, 24 hpi) at an MOI of 0.3, then they were harvested and HMGB1 protein and EV71 VP1 protein was evaluated by Western blot assay, normalized to β-actin. The intensity of Western blot bands signals was quantified by Image J software **(C). (D)** HT-29 cells were infected with EV71 (0, 12, 24, 36 hpi) at an MOI of 1, then cells were harvested and the HMGB1 mRNA levels were quantified by quantitative real-time PCR, normalized against GAPDH. **(E)** HT-29 cells were infected with EV71 (0, 12, 24, 36 hpi) at an MOI of 1, then the cells were harvested and HMGB1 protein and EV71 VP1 protein was measured by Western blot assay, normalized to β-actin. The intensity of Western blot bands signals was quantified by Image J software **(F). (G)** HeLa cells were infected with EV71 (0, 8, 16, 24 hpi) at an MOI of 0.3, then culture supernatants were collected and subjected to ELISA to analyze HMGB1 release. **(H)** HT-29 cells were infected with EV71 (0, 12, 24, 36 hpi) at an MOI of 1, then culture supernatants were collected and subjected to ELISA to analyze HMGB1 release. **(I)** HT-29 cells were uninfected (Mock) or EV71 (MOI = 1) infected for 12 h, then cells were fixed for immunostaining using HMGB1 antibody (red) and EV71 VP1 antibody (green) (in the left). Nuclei were labeled with DAPI (blue). Scale bars, 10 μm. The percentage of cells with altered HMGB1 localization (nuclear or cytoplasm) in EV71 or Mock groups was quantified (in the right). n = 5. The yellow box indicated a partial zoom of the sections and the yellow * showed the cytoplasmic localization of HMGB1 in EV71-infected cells. Data are shown as the mean ± SEM (ns, no significant, $^{*}P < 0.05$, $^{**}P < 0.01$, $^{***}P < 0.001$, $^{****}P < 0.0001$).

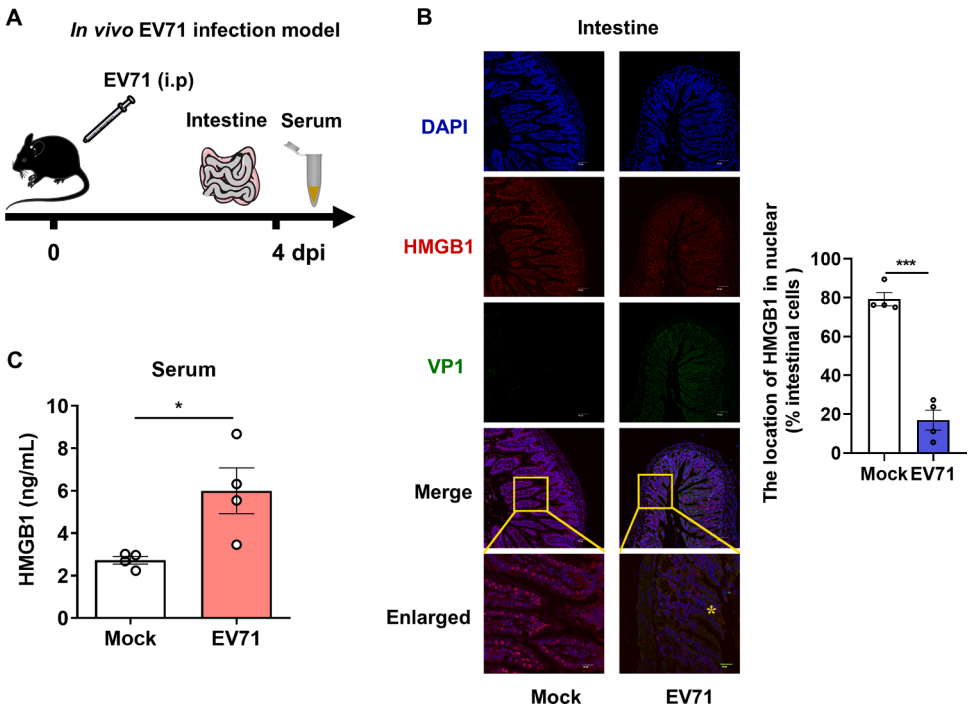

Fig. 2. HMGB1 release is induced by EV71 infection *in vivo*.
(A) Two-week-old AG6 mice (n = 4) were inoculated intraperitoneally with EV71 at 1.76×10^7 PFU/mouse. Then mice were sacrificed at 4 dpi; the small intestine tissues were harvested for immunofluorescent staining and the serum samples were collected for ELISA assay. **(B)** The intestine tissue sections from Mock-infected or EV71-infected mice were immunostained with antibodies against HMGB1 (red) and EV71 VP1 (green) (in the left). The nuclei were stained with DAPI (blue). Scale bars, 50 μm. The yellow box indicated a partial zoom of the sections and the yellow * showed the cytoplasmic localization of HMGB1 in EV71-infected intestine tissue. Scale bars, 20 μm. The percentage of intestinal cells with nucleus-localized HMGB1 in the EV71-infected or Mock-infected mice was quantified (in the right). **(C)** HMGB1 levels in serum from Mock or EV71-infected mice were assessed by ELISA assay. Data are shown as the mean ± SEM (*$P < 0.05$, ***$P < 0.001$).

HMGB1 protein in our *in vivo* BBB model (Fig. 4**F**). After 7 days, EV71 induced 1.8-fold increased leakage in brain vessels of mice as compared to mock group, and stimulation with HMGB1 protein either alone or in the presence of viral infection resulted in a significant increase in BBB permeability in mice (Fig. 4**G**).

To evaluate the extent of CNS inflammation, we monitored GFAP-labeled astrocytes and Iba1-labeled microglia. We found that astrocytes and microglia were significantly increased in the cerebral cortex of EV71-infected mice, and the addition of HMGB1 stimulation with EV71 infection markedly increased the number of activated astrocytes by approximately 16.3-fold, but not the microglia (Fig. 4**H**), which indicated that CNS inflammation was exacerbated after HMGB1 stimulation.

3.4. Released HMGB1 enhances VE-cadherin phosphorylation to disrupt BBB integrity

The proteins of TJs and AJs, including VE-cadherin, Claudin-5, Occludin, ZO-1, played an pivotal role in maintaining the integrity of the BBB. At present, we found that EV71 infection increased VE-cadherin by 1.6-fold and decreased Claudin-5 by 24% (Fig. 5**A**). Occludin and ZO-1 levels were not affected in EV71 infection (Fig. 5**A**). To our surprise, HMGB1 stimulation (500 ng/mL) substantially reduced the levels of VE-cadherin induced by EV71 infection, but not Claudin-5 (Fig. 5**A**). VE-cadherin usually regulates vascular barrier integrity via affecting paracellular permeability, and VE-cadherin phosphorylated at Tyr^{685} is normally internalized, leading to impaired adhesion function of VE-cadherin. (Xu et al., 2021, Li et al., 2018) We found that VE-cadherin phosphorylation at Tyr^{685} increased by 26% and 46% when stimulated with 50 ng/mL and 500 ng/mL HMGB1 during EV71 infection, respectively (Fig. 5**B** and **C**). After treatment with anti-HMGB1 neutralizing antibody, the expression of phosphorylated-VE-cadherin at Tyr685 was significantly reduced (Fig. 5**D** and **E**), and VE-cadherin protein levels were also restored (Fig. 5**D** and **F**).

We also explored the VE-cadherin levels in our *in vivo BBB model*, and found that HMGB1 stimulation significantly reduced total VE-cadherin levels (~70%) in the cerebral cortex of EV71-infected mice as shown in Fig. 5**G**, which is consistent with our *in vitro* results. Overall, these results indicated that HMGB1 release induced by EV71 disrupted the BBB intensity through increasing VE-cadherin phosphorylation, leading to reduction of VE-cadherin.

4. Discussion

Since the discovery of HMGB1 as a late proinflammatory factor in sepsis, HMGB1 has been recognized as a damage-associated molecular pattern (DAMP) in multiple diseases. (Deng et al., 2022) We explored the role of HMGB1 in EV71 infection, and found that HMGB1 mRNA levels were elevated and HMGB1 protein was released to response to viral infection. And the dynamics of HMGB1 suggested that EV71 promoted the HMGB1 cytoplasmic translocation and then released into the extracellular space *in vitro* and *in vivo*. HMGB1 performs distinct biological functions intracellularly and extracellularly, and intracellular HMGB1 mainly regulates viral replications. (Yu et al., 2015, Kagele et al., 2012, Moisy et al., 2012) Once released outside the cell, HMGB1 activated innate immune pathways and induced the expression of interferons and inflammation cytokines in viral infection. (Qu et al., 2018, Jung et al., 2011) However, EV71 has developed multiple escape strategies against innate immunity: the protease 2A of EV71 was involved in affecting IRF3 (interferon regulatory factor) signaling, thereby inhibiting the production of IFN-α/β. (Feng et al., 2014) Reduction of IFNAR1 (type I IFN receptor) induced by $2A^{pro}$ blocked IFN-mediated phosphorylation of Tyk2, Jak1, STAT1 and STAT2 in EV71 infection. (Lu et al., 2012) Thus, the lack of effect of released HMGB1 on EV71 replication is perhaps due to EV71 evading natural immunity.

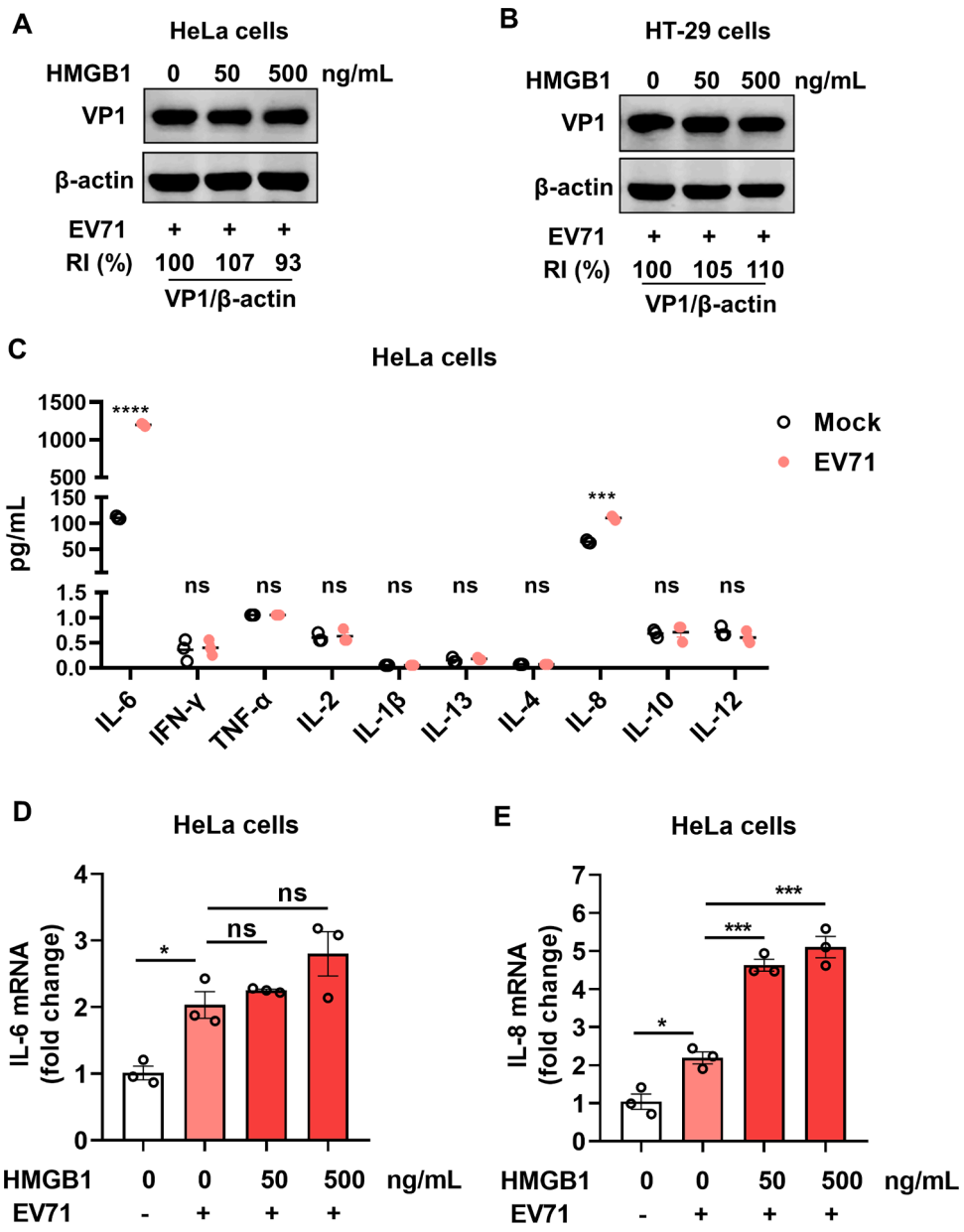

Fig. 3. Released HMGB1 increases IL-8 expression.
(A) HeLa cells were infected with EV71 at an MOI of 0.3 in the presence of different concentrations of recombinant HMGB1 protein for 24 h. The cells were harvested and EV71 VP1 protein was evaluated via Western blot assay, normalized to β-actin. RI, relative intensity. **(B)** HT-29 cells were infected with EV71 at an MOI of 1 in the presence of different concentrations of recombinant HMGB1 protein for 24 h. The cells were harvested and the HMGB1 protein and EV71 VP1 protein was evaluated via Western blot assay, normalized to β-actin. **(C)** HeLa cells were infected with EV71 at an MOI of 0.3 for 24 h, then the culture supernatants were collected for ELISA analyzing. **(D** and **E)** HeLa cells were infected with EV71 at an MOI of 0.3 in the presence of different concentrations of recombinant HMGB1 protein for 24 h, then the cells were harvested and the IL-6 mRNA levels and IL-8 mRNA levels were quantified by quantitative real-time PCR, normalized against GAPDH. Data are shown as the mean ± SEM (ns, no significant, $^{*}P < 0.05$, $^{***}P < 0.001$, $^{****}P < 0.0001$).

Extensive studies have shown that released HMGB1 strongly induces proinflammatory cytokines expression. (Wang et al., 1999, Ding et al., 2021, Andersson et al., 2020) We discovered that released HMGB1 increased IL-8 expression in EV71 infection, which is consistent with several different disease models. (Zha et al., 2020, Min et al., 2017, Shimizu et al., 2016) IL-8 is a pro-inflammatory chemokine that induces neutrophil infiltration into the brain and neutrophil-mediated-inflammation. (Zhu et al., 2022) Sun et al. found that IL-8 induced a significant increase in BBB permeability by altering the paracellular barrier and the transcellular barrier, resulting in Streptococcus suis serotype 2 (SS2)-induced meningitis. (Sun et al., 2016) Thus, HMGB1 may enhance the ability to disrupt the BBB and cause CNS inflammation by increasing IL-8 expression.

EV71 infection led to the inflammation occurring in the brain since viral antigens and RNA were detected in the neurons, and a variety of neuroleptic viruses could enter the CNS by destroying the BBB. (Koyuncu et al., 2013, Wong et al., 2008) Therefore, whether EV71 infection resulted in the disruption of BBB and the respective mechanisms of destroying the BBB were explored in our study. We found that EV71 disrupted BBB integrity in both monolayer HCMECs and mice brain, and HMGB1 stimulation apparently accelerated this process. Activated astrocytes and microglia were increased in EV71-infected mice brain, which is consistent with the previous studies about EV71 associated CNS inflammation. (Jin et al., 2021) In addition to inducing

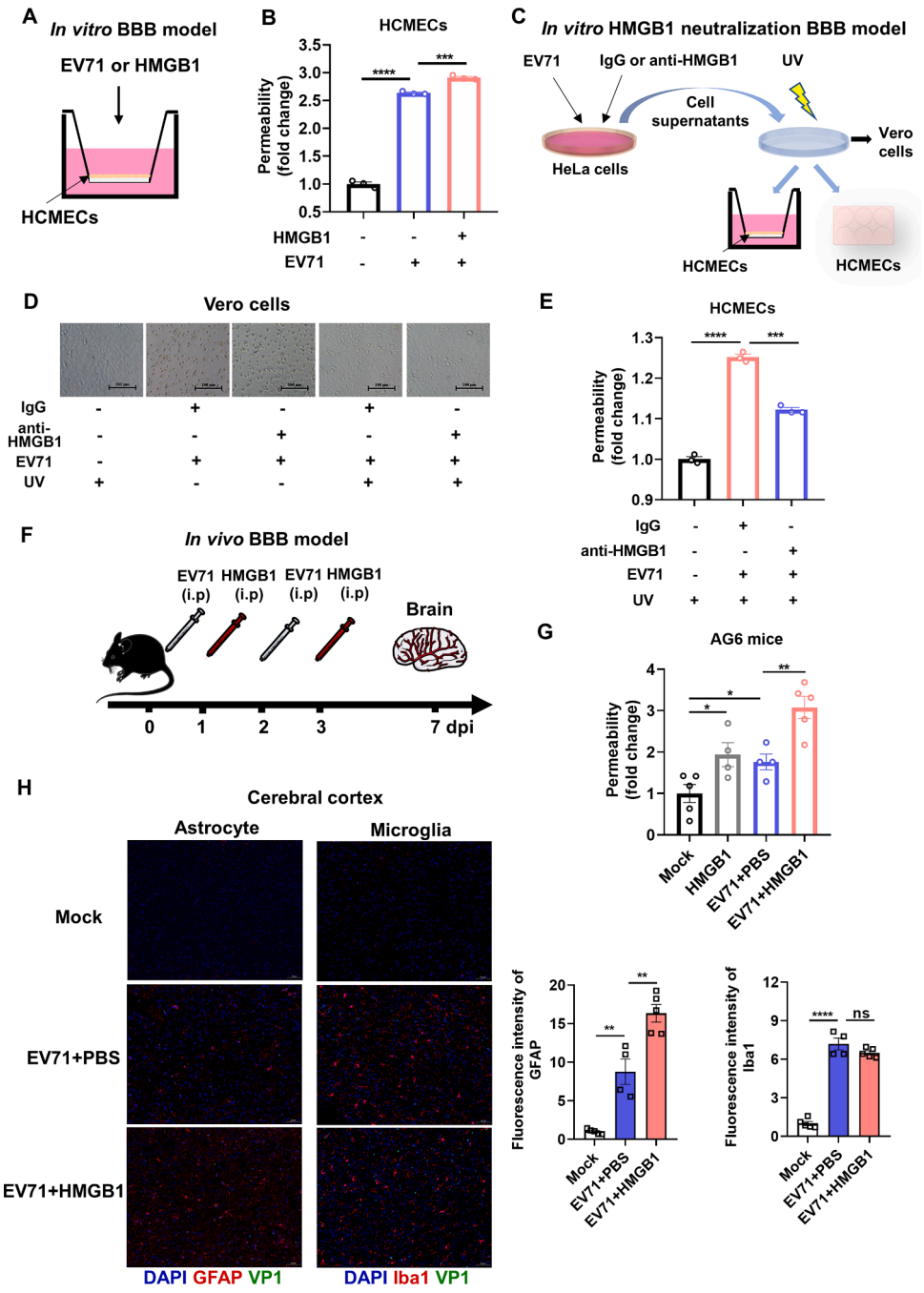

Fig. 4. Released HMGB1 increases EV71-induced BBB permeability and CNS inflammation.
(A) The *in vitro* BBB model. HCMEC monolayer cells were treated with EV71 (3.12×10^6 PFU/well) or HMGB1 protein (1.25 ug/well) for 24 h, then the permeability of HCMEC monolayer cells was measured. **(B)** The permeability of HCMEC monolayer cells in *in vitro* BBB model was measured by sodium fluorescein leakage experiment. The permeability of untreated group was considered as control. **(C)** The *in vitro* HMGB1 neutralization BBB model. HeLa cells were infected with EV71 (MOI = 0.3) in the presence of anti-HMGB1 neutralizing antibody (2.5 ug/mL) or control IgG antibody. After 24 h, the cell supernatants were collected and then treated with UV for 30 min in sterile dish. Then, the UV-treated cell supernatants were added to Vero cells, HCMEC monolayer cells in *in vitro* BBB model and HCMECs in 6-well plates. **(D)** The cell supernatants in *in vitro* HMGB1 neutralization BBB model were added to Vero cells. After 24 h, the morphological images of Vero cells were recorded. Scale bars, 100 μm. **(E)** The permeability of HCMEC monolayer cells in *in vitro* HMGB1 neutralization BBB model was measured by sodium fluorescein leakage experiment. **(F)** The *in vivo* BBB model. Two-week-old AG6 mice (n = 4 or 5) were inoculated intraperitoneally with EV71 at 1.76×10^7 PFU/mouse and stimulated with PBS or HMGB1 protein at 5 μg/mouse. Mice were sacrificed at 7 dpi, then the permeability of BBB was measured, the rest brain tissues were harvested for immunofluorescent staining. **(G)** The permeability of BBB in *in vivo* BBB model was measured by Evens blue leakage experiment. **(H)** Lossy sections of brain from Mock group, EV71-infected with PBS-treated mice or EV71-infected with HMGB1 protein-stimulated mice were immunostained with antibodies against GFAP (red), Iba1 (red) and EV71 VP1 (green), respectively (in the left). The nuclei were stained with DAPI (blue). Scale bars, 50 μm. The fluorescence intensity of GFAP or Iba1 in cerebral cortex was quantified by Image J software (in the right). Data are shown as the mean ± SEM (ns, no significant, $^*P < 0.05$, $^{**}P < 0.01$, $^{***}P < 0.001$, $^{****}P < 0.0001$).

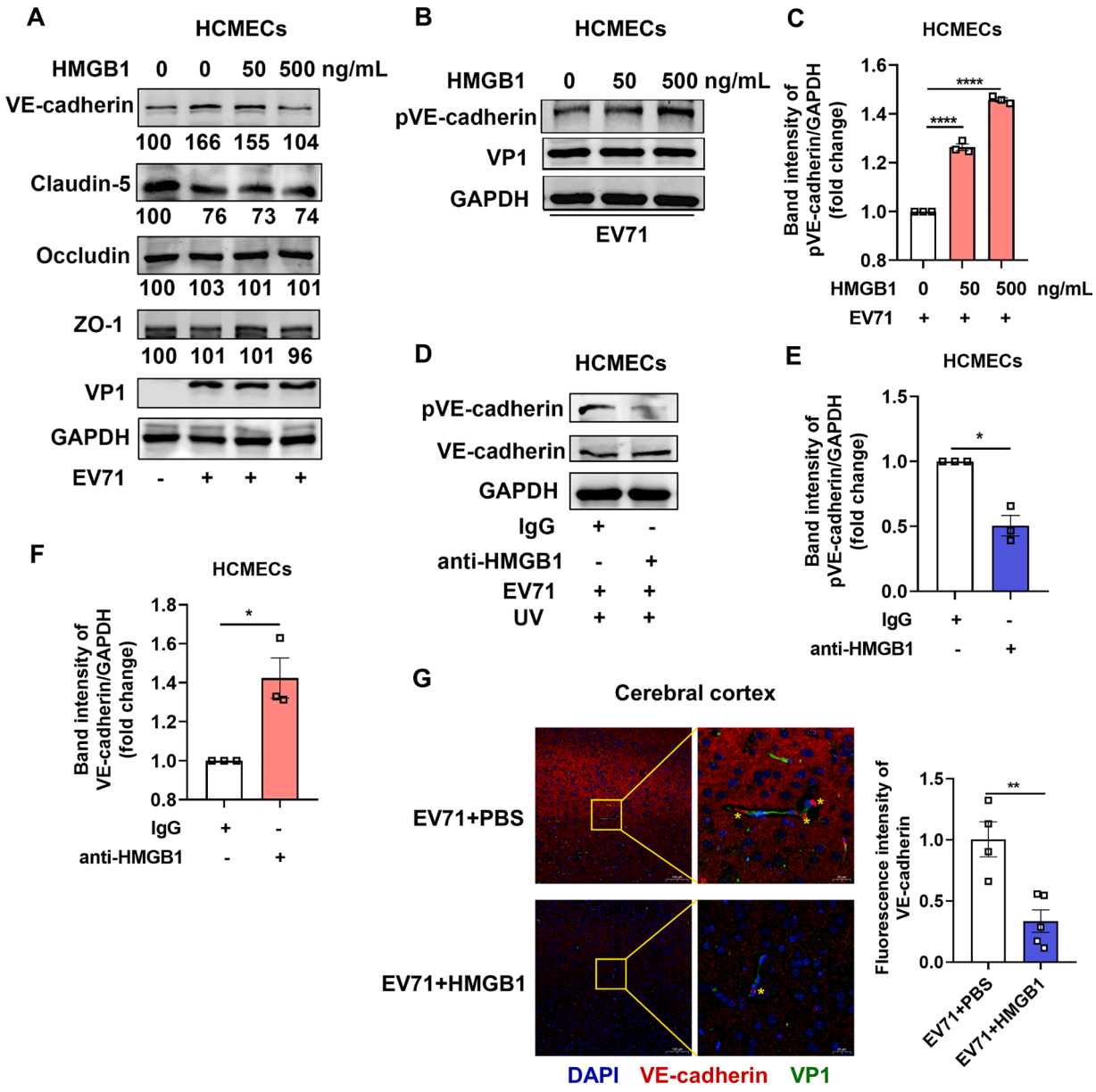

Fig. 5. Released HMGB1 enhances VE-cadherin phosphorylation.
(A) HCMECs were uninfected or infected with EV71 (MOI = 0.5) for 24 h in the presence of different concentrations of HMGB1 protein (0, 50, 500 ng/mL). Then the cells were harvested and the protein levels of VE-cadherin, Claudin-5, Occludin, ZO-1, VP1 were evaluated via Western blot assay, normalized to GAPDH. The band intensity of proteins was quantified by Image J software. **(B)** HCMECs were infected with EV71 (MOI = 0.5) for 24 h in the presence of different concentrations of HMGB1 protein (0, 50, 500 ng/mL). And the cells were harvested and the protein levels of phosphorylation of VE-cadherin Tyr^{685} and EV71 VP1 were evaluated via Western blot assay, normalized to GAPDH. The band intensity of phosphorylation of VE-cadherin Tyr^{685} was quantified by Image J software **(C). (D)** The cell supernatants in *in vitro* HMGB1 neutralization BBB model were added to HCMECs for 24 h. Then the cells were harvested and the protein levels of phosphorylation of VE-cadherin Tyr^{685}, VE-cadherin were evaluated via Western blot assay, normalized to GAPDH. The band intensity of phosphorylation of VE-cadherin Tyr^{685} or VE-cadherin was quantified by Image J software **(E** and **F). (G)** Lossy sections of brain from EV71-infected with PBS-treated mice or EV71-infected with HMGB1 protein-stimulated mice were immunostained with antibodies against VE-cadherin (red) and EV71 VP1 (green), respectively (in the left). The nuclei were stained with DAPI (blue). Scale bars, 100 μm. The yellow box indicated a partial zoom of the sections. The yellow * showed the VE-cadherin. Scale bars, 20 μm. The fluorescence intensity of VE-cadherin in cerebral cortex was quantified by Image J software (in the right). Data are shown as the mean ± SEM (*$P < 0.05$, **$P < 0.01$, ****$P < 0.0001$).

inflammatory responses in the CNS, astrocytes form the outer layer of mature capillaries that help maintain the BBB. (Linnerbauer et al., 2020, Zhao et al., 2015) In our study, astrocytes rather than microglia were response to HMGB1 stimulation, indicating that peripheral blood-derived HMGB1 may be more inclined to activate astrocytes. The mechanisms regarding HMGB1-induced astrocyte activation for BBB maintenance will be worth exploring.

VE-cadherin is the major and specific component of endothelial adhering junctions. (Dejana and Orsenigo, 2013) Our present results indicated that HMGB1 destabilized the interactions between the endothelial cells and weaken the function of vascular barrier via increasing VE-cadherin phosphorylation at Tyr^{685} and reducing total VE-cadherin levels. However, the signaling pathways involved are not well understood. It has been reported that activation of Src (proto-oncogene tyrosine protein kinase Src) modulated Tyr^{685} phosphorylated VE-cadherin-induced vascular permeability. (Orsenigo et al., 2012) Dan

et al. reported that 500 ng/mL HMGB1 stimulation strongly induced phosphorylation-mediated activation of Src, and silencing RAGE (advanced glycation end products, the HMGB1-specific receptor on endothelial cells) blocked HMGB1-induced Src phosphorylation. In our study, we also found that RAGE but not TLR4 (one of the HMGB1 receptors), was 1.5-fold upregulated induced by EV71 infection in the presence of HMGB1 protein (**Figure S1D**), which indicate that RAGE may mediate HMGB1-induced phosphorylation of VE-cadherin.

While vaccines are available for the prevention of EV71-caused HFMD, there are currently no approved drugs to treat the neurological damage in HFMD patients. (Nguyen et al., 2022) HMGB1 is considered a therapeutic target for the treatment of inflammatory diseases, and many HMGB1 antagonists have been identified including anti-HMGB1 neutralizing antibody and HMGB1 release inhibitors ethyl pyruvate and glycyrrhizin. (Xue et al., 2021) Treatment with anti-HMGB1 neutralizing antibody remarkably ameliorated intracerebral hemorrhage-injury by protecting BBB integrity and decreasing activated microglia and the expression of inflammation-related factors in rats. (Wang et al., 2017) Application of ethyl pyruvate + glycyrrhizin treatment reduced Alzheimer's disease and frontotemporal dementia associated pathological tau oligomers-induced neuroinflammation and cognitive dysfunction in mice. (Gaikwad et al., 2021) However, the therapeutic role of anti-HMGB1 neutralizing antibody in EV71-induced BBB disruption has not been adequately evaluated in our study. Therefore, future evaluation of the BBB-protecting role of anti-HMGB1 neutralizing antibody is of great interest. And evaluating the efficacy of HMGB1 antagonists in HFMD animal models and HFMD patients will greatly inform the treatment of HFMD caused by EV71.

Author contributions

Qiao You, Jing Wu, Deyan Chen, Ye Liu, Fang Zhang: conceptualization, methodology, software, data curation and writing-original draft. **Na Jiang, Xiaoyan Tian, Yurong Cai, Enhui Yang, Ruining Lyu, Nan Zheng:** methodology, data curation and visualization. **Zhiwei Wu:** funding the project, reviewing and editing the manuscript. All authors critically reviewed the manuscript and approved the final version.

Declaration of Competing Interest

The authors declare that they have no known competing financial interests or personal relationships that could have appeared to influence the work reported in this paper.

Data availability

Data will be made available on request.

Acknowledgments

This work was supported by the National Natural Science Foundation of China (81900823 to C.D.Y, and U22A20335 and 31970149 to W.Z.W.), the Major Research and Development Project (2018ZX10301406 to W.Z.W.) and Nanjing University-Ningxia University Collaborative Project (2017BN04 to W.Z.W.).

Supplementary materials

Supplementary material associated with this article can be found, in the online version, at doi:10.1016/j.virusres.2023.199240.

References

Andersson, U, Ottestad, W, Tracey, KJ., 2020. Extracellular HMGB1: a therapeutic target in severe pulmonary inflammation including COVID-19? Mol Med 26 (1), 42.
Andersson, U, Tracey, KJ., 2011. HMGB1 is a therapeutic target for sterile inflammation and infection. Annu Rev Immunol 29, 139–162.
Chang, LY, Huang, LM, Gau, SS, et al., 2007. Neurodevelopment and cognition in children after enterovirus 71 infection. N Engl J Med 356 (12), 1226–1234.
Chen, D, Feng, C, Tian, X, Zheng, N, Wu, Z., 2018. Promyelocytic Leukemia Restricts Enterovirus 71 Replication by Inhibiting Autophagy. Front Immunol 9, 1268.
Colombo, E, Farina, C., 2016. Astrocytes: Key Regulators of Neuroinflammation. Trends Immunol 37 (9), 608–620.
Colonna, M, Butovsky, O., 2017. Microglia Function in the Central Nervous System During Health and Neurodegeneration. Annu Rev Immunol 35, 441–468.
Cox, B, Levent, F., 2018. Hand, Foot, and Mouth Disease. JAMA 320 (23), 2492. -2492.
Crabol, Y, Pean, P, Mey, C, et al., 2017. A prospective, comparative study of severe neurological and uncomplicated hand, foot and mouth forms of paediatric enterovirus 71 infections. Int J Infect Dis 59, 69–76.
Dejana, E, Orsenigo, F., 2013. Endothelial adherens junctions at a glance. J Cell Sci 126 (Pt 12), 2545–2549.
Deng, C, Zhao, L, Yang, Z, et al., 2022. Targeting HMGB1 for the treatment of sepsis and sepsis-induced organ injury. Acta Pharmacol Sin 43 (3), 520–528.
Ding, X, Li, S, Zhu, L., 2021. Potential effects of HMGB1 on viral replication and virus infection-induced inflammatory responses: A promising therapeutic target for virus infection-induced inflammatory diseases. Cytokine Growth Factor Rev.
Feng, C, Fu, Y, Chen, D, et al., 2017. miR-127-5p negatively regulates enterovirus 71 replication by directly targeting SCARB2. FEBS Open Bio 7 (6), 747–758.
Feng, Q, Langereis, MA, Lork, M, et al., 2014. Enterovirus 2Apro targets MDA5 and MAVS in infected cells. J Virol 88 (6), 3369–3378.
Fu, Y, Zhang, L, Zhang, R, et al., 2019. Enterovirus 71 Suppresses miR-17-92 Cluster Through Up-Regulating Methylation of the miRNA Promoter. Front Microbiol 10, 625.
Gaikwad, S, Puangmalai, N, Bittar, A, et al., 2021. Tau oligomer induced HMGB1 release contributes to cellular senescence and neuropathology linked to Alzheimer's disease and frontotemporal dementia. Cell Rep 36 (3), 109419.
Jin, Y, Sun, T, Zhou, G, et al., 2021. Pathogenesis Study of Enterovirus 71 Using a Novel Human SCARB2 Knock-In Mouse Model. mSphere 6 (2).
Jung, JH, Park, JH, Jee, MH, et al., 2011. Hepatitis C virus infection is blocked by HMGB1 released from virus-infected cells. J Virol 85 (18), 9359–9368.
Kagele, D, Rossetto, CC, Tarrant, MT, Pari, GS., 2012. Analysis of the interactions of viral and cellular factors with human cytomegalovirus lytic origin of replication, oriLyt. Virology 424 (2), 106–114.
Koyuncu, OO, Hogue, IB, Enquist, LW., 2013. Virus infections in the nervous system. Cell Host Microbe 13 (4), 379–393.
Li, W, Chen, Z, Chin, I, Chen, Z, Dai, H., 2018. The Role of VE-cadherin in Blood-brain Barrier Integrity Under Central Nervous System Pathological Conditions. Curr Neuropharmacol 16 (9), 1375–1384.
Liebner, S, Dijkhuizen, RM, Reiss, Y, Plate, KH, Agalliu, D, Constantin, G., 2018. Functional morphology of the blood-brain barrier in health and disease. Acta Neuropathol 135 (3), 311–336.
Linnerbauer, M, Wheeler, MA, Quintana, FJ., 2020. Astrocyte Crosstalk in CNS Inflammation. Neuron 108 (4), 608–622.
Lu, J, Yi, L, Zhao, J, et al., 2012. Enterovirus 71 disrupts interferon signaling by reducing the level of interferon receptor 1. J Virol 86 (7), 3767–3776.
Min, HJ, Kim, JH, Yoo, JE, et al., 2017. ROS-dependent HMGB1 secretion upregulates IL-8 in upper airway epithelial cells under hypoxic condition. Mucosal Immunol 10 (3), 685–694.
Moisy, D, Avilov, SV, Jacob, Y, et al., 2012. HMGB1 protein binds to influenza virus nucleoprotein and promotes viral replication. J Virol 86 (17), 9122–9133.
Nguyen, TT, Chiu, CH, Lin, CY, et al., 2022. Efficacy, safety, and immunogenicity of an inactivated, adjuvanted enterovirus 71 vaccine in infants and children: a multiregion, double-blind, randomised, placebo-controlled, phase 3 trial. Lancet 399 (10336), 1708–1717.
Nishibori, M, Mori, S, Takahashi, HK., 2019. Anti-HMGB1 monoclonal antibody therapy for a wide range of CNS and PNS diseases. J Pharmacol Sci 140 (1), 94–101.
Nishibori, M, Wang, D, Ousaka, D, Wake, H., 2020. High Mobility Group Box-1 and Blood-Brain Barrier Disruption. Cells 9 (12).
Nosaka, N, Hatayama, K, Yamada, M, et al., 2018. Anti-high mobility group box-1 monoclonal antibody treatment of brain edema induced by influenza infection and lipopolysaccharide. J Med Virol 90 (7), 1192–1198.
Obermeier, B, Daneman, R, Ransohoff, RM., 2013. Development, maintenance and disruption of the blood-brain barrier. Nat Med 19 (12), 1584–1596.
Ooi, MH, Wong, SC, Lewthwaite, P, Cardosa, MJ, Solomon, T., 2010. Clinical features, diagnosis, and management of enterovirus 71. The Lancet Neurology 9 (11), 1097–1105.
Orsenigo, F, Giampietro, C, Ferrari, A, et al., 2012. Phosphorylation of VE-cadherin is modulated by haemodynamic forces and contributes to the regulation of vascular permeability in vivo. Nat Commun 3, 1208.
Qu, Y, Zhan, Y, Yang, S, et al., 2018. Newcastle disease virus infection triggers HMGB1 release to promote the inflammatory response. Virology 525, 19–31.
Shimizu, S, Kouzaki, H, Kato, T, Tojima, I, Shimizu, T., 2016. HMGB1-TLR4 signaling contributes to the secretion of interleukin 6 and interleukin 8 by nasal epithelial cells. Am J Rhinol Allergy 30 (3), 167–172.
Solomon, T, Lewthwaite, P, Perera, D, Cardosa, MJ, McMinn, P, Ooi, MH., 2010. Virology, epidemiology, pathogenesis, and control of enterovirus 71. The Lancet Infectious Diseases 10 (11), 778–790.

Stros, M., 2010. HMGB proteins: interactions with DNA and chromatin. Biochim Biophys Acta 1799 (1-2), 101–113.
Sun, Y, Li, N, Zhang, J, et al., 2016. Enolase of Streptococcus Suis Serotype 2 Enhances Blood-Brain Barrier Permeability by Inducing IL-8 Release. Inflammation 39 (2), 718–726.
Sweeney, MD, Sagare, AP, Zlokovic, BV., 2018. Blood-brain barrier breakdown in Alzheimer disease and other neurodegenerative disorders. Nat Rev Neurol 14 (3), 133–150.
Sweeney, MD, Zhao, Z, Montagne, A, Nelson, AR, Zlokovic, BV., 2019. Blood-Brain Barrier: From Physiology to Disease and Back. Physiol Rev 99 (1), 21–78.
Wang, D, Liu, K, Wake, H, Teshigawara, K, Mori, S, Nishibori, M., 2017. Anti-high mobility group box-1 (HMGB1) antibody inhibits hemorrhage-induced brain injury and improved neurological deficits in rats. Sci Rep. 7, 46243.
Wang, F, Ji, S, Wang, M, et al., 2020. HMGB1 promoted P-glycoprotein at the blood-brain barrier in MCAO rats via TLR4/NF-κB signaling pathway. Eur J Pharmacol 880, 173189.
Wang, H, Bloom, O, Zhang, M, et al., 1999. HMG-1 as a late mediator of endotoxin lethality in mice. Science 285 (5425), 248–251.
Wang, H, Yuan, M, Wang, S, et al., 2019. STAT3 Regulates the Type I IFN-Mediated Antiviral Response by Interfering with the Nuclear Entry of STAT1. Int J Mol Sci 20 (19).
Wang, H, Yuan, M, Yang, E, Chen, D, Su, A, Wu, Z, 2021. Enterovirus 71 infection induced Aquaporin-4 depolarization by increasing matrix metalloproteinase-9 activity. Neurosci Lett 759, 136049.
Wong, KT, Munisamy, B, Ong, KC, et al., 2008. The distribution of inflammation and virus in human enterovirus 71 encephalomyelitis suggests possible viral spread by neural pathways. J Neuropathol Exp Neurol 67 (2), 162–169.
Xu, S, Jiang, N, Nawaz, W, et al., 2021. Infection of humanized mice with a novel phlebovirus presented pathogenic features of severe fever with thrombocytopenia syndrome. PLoS Pathog 17 (5), e1009587.
Xue, J, Suarez, JS, Minaai, M, et al., 2021. HMGB1 as a therapeutic target in disease. J Cell Physiol 236 (5), 3406–3419.
Yu, R, Yang, D, Lei, S, et al., 2015. HMGB1 Promotes Hepatitis C Virus Replication by Interaction with Stem-Loop 4 in the Viral 5′ Untranslated Region. J Virol 90 (5), 2332–2344.
Zha, C, Meng, X, Li, L, et al., 2020. Neutrophil extracellular traps mediate the crosstalk between glioma progression and the tumor microenvironment via the HMGB1/RAGE/IL-8 axis. Cancer Biol Med 17 (1), 154–168.
Zhang, J, Takahashi, HK, Liu, K, et al., 2011. Anti-high mobility group box-1 monoclonal antibody protects the blood-brain barrier from ischemia-induced disruption in rats. Stroke 42 (5), 1420–1428.
Zhao, Z, Nelson, AR, Betsholtz, C, Zlokovic, BV., 2015. Establishment and Dysfunction of the Blood-Brain Barrier. Cell 163 (5), 1064–1078.
Zheng, W, Shi, H, Chen, Y, Xu, Z, Chen, J, Jin, L, 2017. Alteration of serum high-mobility group protein 1 (HMGB1) levels in children with enterovirus 71-induced hand, foot, and mouth disease. Medicine (Baltimore) 96 (17), e6764.
Zhou, J, Guan, MY, Li, RT, et al., 2023. Zika virus leads to olfactory disorders in mice by targeting olfactory ensheathing cells. EBioMedicine 89, 104457.
Zhu, F, Xu, W, Xia, J, et al., 2014. Efficacy, safety, and immunogenicity of an enterovirus 71 vaccine in China. N Engl J Med 370 (9), 818–828.
Zhu, H, Hu, S, Li, Y, et al., 2022. Interleukins and Ischemic Stroke. Front Immunol 13, 828447.